

Thermal response of Bessel beam-heated microdroplets carrying nanoparticles for deposition

Cite as: J. Laser Appl. **33**, 012043 (2021); <https://doi.org/10.2351/7.0000332>

Submitted: 30 November 2020 . Accepted: 30 November 2020 . Published Online: 15 January 2021

Eduardo Castillo-Orozco, Ranganathan Kumar, and  Aravinda Kar



View Online



Export Citation



CrossMark



The professional society for
lasers, laser applications,
and laser safety worldwide.

Become part of the LIA experience -
cultivating innovation, ingenuity, and
inspiration within the laser community.

Find Out More



www.lia.org/membership
membership@lia.org

Thermal response of Bessel beam-heated microdroplets carrying nanoparticles for deposition

Cite as: J. Laser Appl. **33**, 012043 (2021); doi: [10.2351/7.0000332](https://doi.org/10.2351/7.0000332)
Submitted: 30 November 2020 · Accepted: 30 November 2020 ·
Published Online: 15 January 2021



Eduardo Castillo-Orozco,¹ Ranganathan Kumar,² and Aravinda Kar³ 

AFFILIATIONS

¹Escuela Superior Politécnica del Litoral, ESPOL, Facultad en Ingeniería Mecánica y Ciencias de la Producción, Campus Gustavo Galindo, Km 30.5 Vía Perimetral, P.O. Box 09-01-5863, Guayaquil EC090112, Ecuador

²Department of Mechanical and Aerospace Engineering, University of Central Florida, Orlando, Florida 32816

³CREOL, The College of Optics and Photonics, University of Central Florida, Orlando, Florida 32816

Note: Paper published as part of the special topic on Proceedings of the International Congress of Applications of Lasers & Electro-Optics 2020.

ABSTRACT

Laser-microdroplet interactions influence the quality of nanoparticle deposition on a substrate. When a microdroplet and its impinging spot are heated, the microdroplet can evaporate gently, boil immediately after impingement, or bounces back inhibiting the deposition process. The interaction between a laser and droplets carrying semiconductor and metal nanoparticles is studied for different laser powers. The results indicate that the laser is refocused by the droplets, and deposition of nanoparticles and formation of nanostructures are achieved under certain conditions. On the other hand, when the laser power exceeds a critical value, heating up the substrate at a specific temperature, microdroplets bounce back from the substrate, except for the cases of liquids with low reflectance coefficient and high absorption coefficient, where a new laser-spraying regime is observed.

Published under license by Laser Institute of America. <https://doi.org/10.2351/7.0000332>

INTRODUCTION

Nanoparticles are the fundamental building blocks of nanotechnology. For some technologies, they are the raw material for manufacturing nanostructured devices and materials.^{1,2} However, manipulation of these nanoparticles is difficult and manifests critical challenges. A method to carry and deposit these nanoparticles is nano-electrospray laser deposition (NELD),³ where an aqueous suspension of nanoparticles, i.e., an aqueous ink, is used as a precursor to produce micro- and nanodroplets via electrospray, and a laser beam is used to evaporate the liquid and simultaneously sinter the nanoparticles. In this method, droplets interact with a laser beam as they are ejected from a nozzle and subsequently impinge on a laser-heated substrate. Collision of droplets on hot surfaces is not limited to this application, but there are several additional applications, such as spray cooling of hot materials, spray coating, combustion engines, etc.,⁴ where understanding of the thermal response of liquid droplets is important.

The dynamics and the thermal response of a droplet's impact on hot surfaces have been extensively investigated in the past.⁵⁻⁷ In most of the studies, droplets larger than 1 mm were used. Nevertheless, much smaller droplets are present in most of the relevant aforementioned technologies. Moreover, it is not completely understood whether the phenomena are similar for larger droplets and smaller droplets.

It is commonly accepted⁸⁻¹¹ that the dynamics of a droplet impacting a hot surface depends heavily on the ratio of the inertia and the surface tension of the liquid droplet, which is described by its Weber number and the temperature of the hot surface. The Weber number is defined as $We = \rho U^2 d / \sigma$, where ρ , U , d , and σ are the density of the liquid, speed of the droplet when it impacts on the surface, diameter of the droplet, and surface tension of the liquid, respectively. Since the We number relates to the droplet's kinetic energy, this parameter affects the behavior of collision. For low We number, the droplet impacts the surface without

disintegration, while for high We number, the droplet disintegrates and splashes, releasing secondary fragments of liquid. On the other hand, the temperature of the substrate is another key parameter since it affects the droplet thermal response. Phenomena such as contact boiling, film boiling, transition boiling, nucleate boiling, and film evaporation have been observed as a function of a variation of the surface temperature of a solid substrate.^{12–14}

Chandra and Avedisian⁶ studied the impingement of n-heptane droplets on a hot stainless steel substrate at temperatures between 24 and 250 °C and a fixed impact We number of 43. Tran *et al.*¹¹ experimentally determined the dependence of the temperature at which the evaporation time of a drop reaches its maximum (Leidenfrost temperature) on impact conditions. They used water drops with ~2 mm diameter and Fluorinert liquid, FC-72 drops with ~1 mm diameter and a temperature variation of a silicon substrate between 200 and 600 °C. Bernardin *et al.*¹² constructed a regime map showing film boiling, transition boiling, nucleate boiling, and film evaporation for impingement of water drops at We numbers 20, 60, and 80 on a hot aluminum substrate at temperatures between 100 and 2080 °C. There are much fewer studies where smaller droplets have been used to investigate these phenomena; however, certain information is available in works by Karl and Frohn⁹ and Chaves *et al.*¹³ Moreover, Fujimoto *et al.*¹⁰ present a detailed review of the literature on the droplet's impact upon hot surfaces.

In most of the studies performed to investigate the outcomes in a droplet impingement problem, homogeneous liquids have been used as well as uniform heating of the substrate via thermal resistances installed within the substrate. Here, we use laser radiation assuming the irradiation intensity of a Bessel beam due to its tight focusing properties to heat up a localized spot of diameter 285 μm to investigate the thermal response of microdroplets of diameter ~70 μm that carry semiconductor and metal nanoparticles for inkjet printing applications. Understanding of the dynamics of the impact of microdroplets, substrate-temperature response, and the laser power effect on the impingement of droplets is important for the deposition and sintering of nanoparticles for the fabrication of nanostructured devices.^{15,16}

EXPERIMENTAL PROCEDURE

Figures 1 and 2(a) show the experimental setup used to perform this study and its schematic representation, respectively. Droplets are formed by forcing an aqueous suspension of nanoparticles (Table I) from a syringe pump at a flow rate of 10 $\mu\text{l}/\text{min}$ through a stainless steel flat-tipped hypodermic needle, i.e., a capillary tube of inner and outer diameters of 0.51 and 0.82 mm, respectively [Fig. 1(a)]. The separation of the needle tip from the substrate surface (the silicon wafer with an average surface roughness of ~5 nm) is 8 mm. This height does not permit the impact kinetic energy to shatter the impacting droplet. Additionally, an electrostatic field is created by applying 3200 V between the needle and the substrate, which work as electrodes. Subsequently, microdroplets ranging from an original preimpact diameter of 75–80 μm , i.e., volumes between 220 and 270 PL (Table I), are generated using this electrospray method and are guided by electric and gravity forces toward a hollow conical laser beam. Eventually, the droplets interact with the laser slightly above or at the substrate surface

[Fig. 2(b)]. In the focal volume, the conical beam forms a Bessel beam irradiation distribution with a focal spot diameter of 285 μm that is used to heat the microdroplet and the droplet-impingement spot. This beam is produced by using an axicon lens and biconvex lens to shape an Nd:YAG Gaussian laser of wavelength 1064 nm [Fig. 1(b)] into an annular beam [Fig. 1(c)], which is later converted by a parabolic mirror into a hollow conical beam. The laser system was operated at a pulse repetition rate of 30 kHz and a pulse length of 170 ns. The laser power was varied between 1 and 30.5 W, in order to change the surface temperature of the silicon substrate. The laser beam was stationary while the substrate was moved at a speed of 0.1 mm/s by a motorized linear transition stage. Thermography (FLIR SC5000 IR-camera) was used to measure the focal spot temperature. High speed imaging (Phanton V12.1 camera) and image processing (in-house Matlab code) were used to analyze the thermal response of the microdroplets to laser heating when the laser power is increased.

RESULTS

Results of this study suggest that at the impact of a nanosuspension microdroplet onto a smooth rigid surface that is heated above the boiling point of the liquid, the microdroplet either instantly boils after collision on the surface, i.e., contact boiling of the microdroplet occurs, or without any contact with the surface develops a Leidenfrost vapor layer beneath the liquid surface and bounces back. On the other hand, if the localized temperature of the droplet-impingement spot is below the boiling point, the nanosuspension microdroplet spreads radially forming a film that gently evaporates, i.e., heating of a sessile microdroplet.

Figure 3 shows (a) the stretching of the electrified meniscus and the formation of monodisperse microdroplet and the interaction between the hydrodynamic forces, i.e., inertial, viscous, and interfacial force; and the electric force detaches a small volume of liquid drop compared to the size of the needle.^{17,18} (b) Histogram of the radius of ejected microdroplets for surfactant solution containing no nanoparticles. The radius of these droplets ranges from 10 to 70 μm with an average size and standard deviation of 36.3 and 9.3 μm , respectively. (c) Sequence of the photograph showing the impingement of various microdroplets on the substrate at laser power 3.5 W and 52.9 °C. The droplet-laser interaction at this laser power and substrate temperature allows the droplets to assume the shape of flattened disks, i.e., a sessile droplet. These droplets are patterned as a linear array by moving the substrate. (d) The temporal view of the laser-droplet interaction as the droplet travels toward the silicon substrate for a laser beam input power of 17 W and diameter of 285 μm on the substrate surface at 102 °C. The interaction of the characteristic cross section intensity of the Bessel beam and the curved liquid surfaces (ripples) due to active boiling of the droplet can be seen as bright spots (fringes) in some of the photographs captured with a high-speed camera operating at the spectral range of 350–950 nm. The fringes were visible only during the time the pulsed laser was on. The brighter spots inside the droplet suggests that the laser beam was refocused by the multiple ripples of small radii of curvature at the surface of the liquid.³ (e) Temporal view of a bouncing droplet on the surface of the silicon substrate at 137 °C for laser input power of 22 W. When the laser

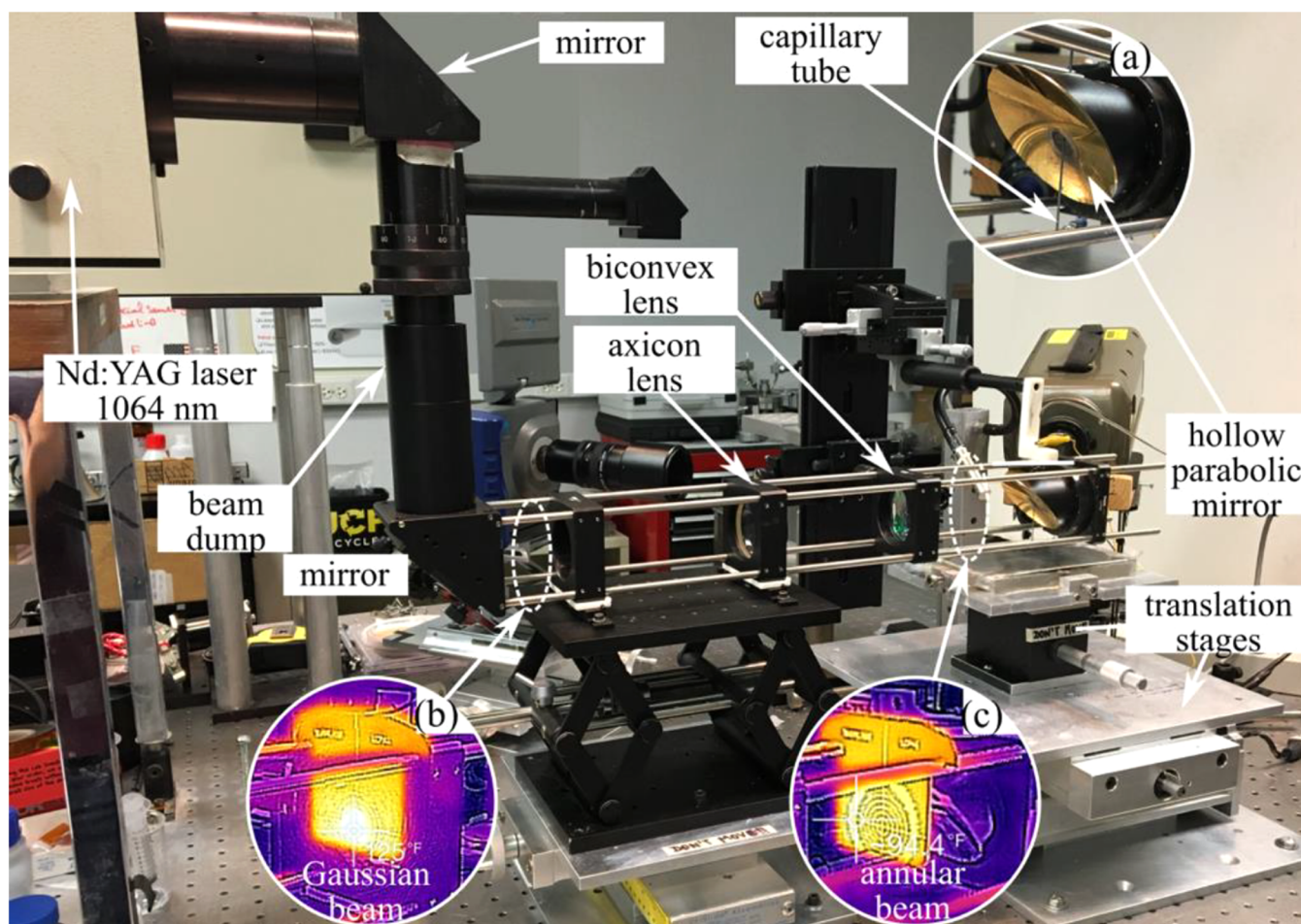


FIG. 1. Experimental setup. (a) Configuration of the capillary tube and the hollow parabolic mirror that allows droplet impingement at the laser beam focal spot. (b) Thermography of the incoming Gaussian laser beam. (c) Thermography of the annular beam.

power exceeds a critical value of ~ 20 W for this case, all microdroplets generated by the electro spray bounce back from the substrate.

Above the critical laser power, the substrate surface is excessively heated by the laser and the interfacial tension at the substrate-droplet interface changes significantly, resulting in a restricted spreading of the droplets on the substrate as it spreads upon impact of the substrate. However, due to changes in the surface tension at high substrate temperatures, the droplet spreads partially with a minimal deformation of the original spherical shape of the incident droplet and subsequently retracts back to its original shape and bounces in the upward direction. The combined effect of this stored energy and the surface tension pulls back the spreading droplet to its original shape. The upward bouncing of the droplets is due to localized rapid evaporation of the liquid at the point of contact between the droplet and the substrate, resulting in the Leidenfrost effect.^{19,20} Rapid vaporization causes the

accumulation of vapor underneath the deformed droplet and builds up pressure that ultimately propels the droplet upward.

Figure 4 shows a regime plot of the different outcomes observed when the liquids listed in Table I, i.e., a surfactant solution, suspensions of Si, Ge, and Ag at different concentrations were tested at various localized surface temperatures of the substrate. This phase diagram shows four different outcomes depending on the power absorbed by the microdroplets and the surface temperature of the substrate. Square markers represent the cases where no boiling of droplet was observed, i.e., the regime: heating of sessile microdroplet. The circles represent the cases where contact boiling was observed. The triangles represent the cases where microdroplets bounced back from the substrate, i.e., the droplet rebound regime. Finally, a fourth regime that was only observed for microdroplets formed from a suspension of Ag with a weight concentration of 20 wt.%. In this regime, the original microdroplets did not reach the substrate to interact directly with the heated substrate, but instead, the laser

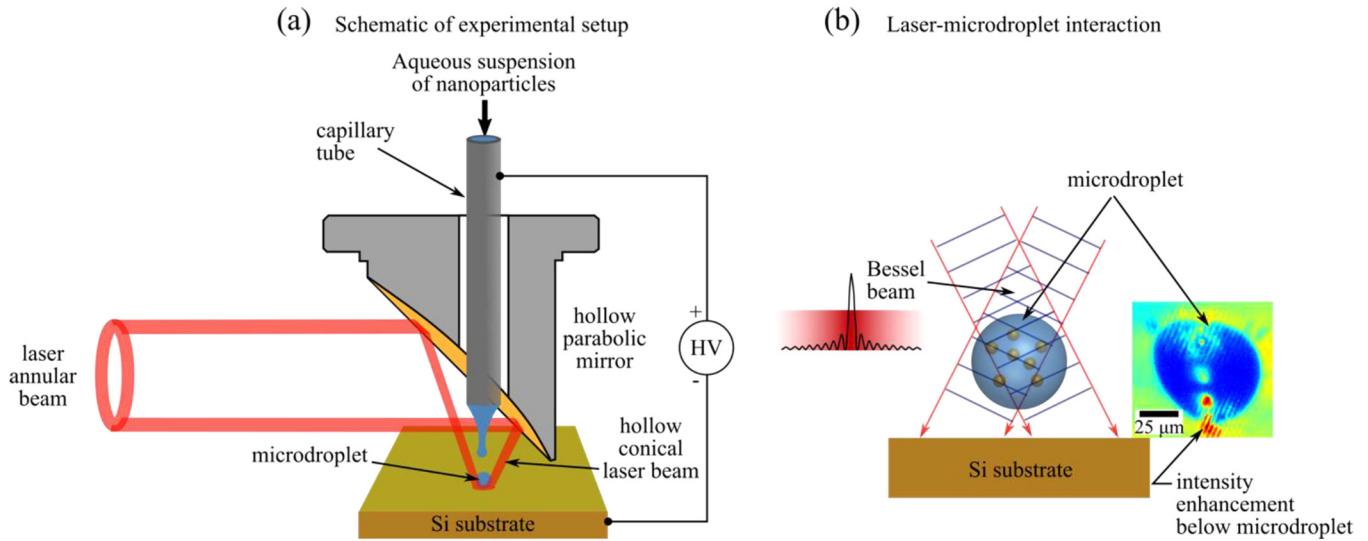


FIG. 2. Schematic of the experimental setup showing the interaction between the laser and the microdroplet. (a) Hollow conical laser beam is focused onto the microdroplet that is generated via electro spray. (b) Interaction between the Bessel laser beam and the microdroplet. The microdroplet acts as a lens enhancing the intensity below the liquid surface.

transferred heat to the microdroplet while it was still in the air at a high enough rate that caused the disruption of the liquid outer surface. This disruption, sometimes even explosive, disintegrated the original droplet and ejected tinier liquid ligaments in the form of a spray. This regime is named in this study as the laser-spraying regime and was not observed in the rest of fluids tested.

DISCUSSION

An ideal Bessel beam can be represented by

$$E(r, \theta, z) = E_0 J_n(k_r r) \exp(ik_z z) \exp(\pm in\theta), \quad (1)$$

where J_n is the n th-order Bessel function of the first kind; k_r and k_z are the radial and longitudinal wavevectors; $k = [k_r^2 + k_z^2]^{1/2} = 2\pi/\lambda$ is the wavevector; λ is the wavelength; and $r, \theta,$ and z are the radial, azimuthal, and longitudinal components, respectively.^{21,22} The intensity profile of a zeroth-order Bessel beam decays at the rate $\sim(k_r r)^{-1}$. However, the time-averaged intensity of

the beam can be described by

$$I(r, \theta, z \geq 0) = |J_0(k_r r)|^2, \quad (2)$$

where $k_r = 2\pi \sin(\theta)/\lambda$ and θ is the opening angle of the cone. Furthermore, it is only a portion of the beam's power that is absorbed by the microdroplet. The expression of the overall power absorbed by the microdroplet is shown in the following equation:

$$P_{abs} = \int_0^{r_0} \int_0^{h(r)} P_0 I(r) (1 - R) \times e^{-\mu z} 2\pi r \, dr dz. \quad (3)$$

However, this is the very general form, integrating in the z direction,

$$P_{abs} = \int_0^{r_0} P_0 I(r) (1 - R) (1 - e^{-\mu h(r)}) 2\pi r \, dr, \quad (4)$$

where R and μ are the reflectance and absorption coefficient if the

TABLE I. Physical properties and relevant parameters of nanoparticles suspensions in DI water.

Nanoparticle suspension in DI water	Density	Viscosity	Surface tension	Reflectance at $\lambda = 1064$ nm	Absorption coefficient at $\lambda = 1064$ nm	Preimpact droplet diameter (average)	Impact Weber number (average)
	(g/ml)	(10^{-3} Pa s)	(10^{-3} N/m)	(%)	(cm^{-1})	(μm)	(—)
Surfactant solution	1.000	1.10	49.8	48	0.2	76.6	0.38
Germanium, 5 wt. %	1.064	1.56	47.5	42	4.17	75.8	0.42
Germanium, 10 wt. %	1.130	1.95	47.6	35	7.7	75.4	0.45
Silicon, 5 wt. %	1.033	1.82	48.2	28	6.25	79.6	0.43
Silver, 20 wt. %	1.153	1.71	47.2	6	100	80.6	0.49

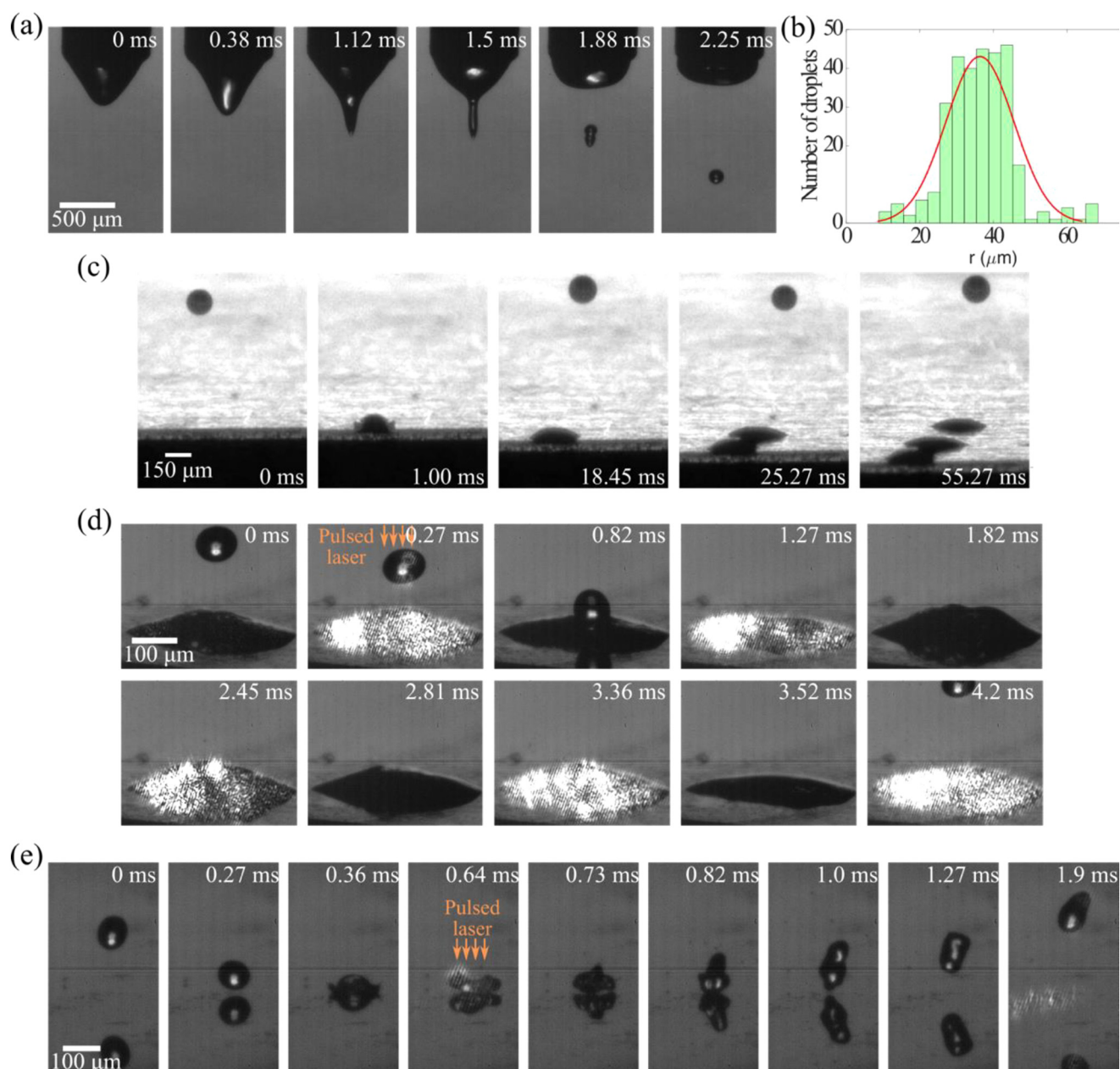


FIG. 3. High-speed imaging of the microdroplet-laser interaction. (a) Droplet formation from the needle under the action of an electric field, 3200 V. Electro spray operated in the microdripping mode. (b) Histogram of radius of microdroplets generated from the electro spray for dl water with surfactant concentration. Average droplet radius of $36.3\ \mu\text{m}$ (mean value) and standard deviation of $9.3\ \mu\text{m}$. (c) Sequence of droplet impingement and laser interaction at a laser power of 3.5 W. Microdroplets spread on the surface to obtain the shape of flattened disks with minimum liquid evaporation. (d) Sequence of droplet impingement and laser interaction at a laser power of 17 W. The impinging droplet boils due to laser heating and heat conduction from the substrate. (e) Rebound of droplet when the laser power is increased at 22 W.

droplet at the wavelength of the laser, P_0 is related to the input energy with $P_0 = P_{in} / \int_0^{r_0} I(r) 2\pi r dr$, and $h(r)$ and r_0 are the depth of the droplet as a function of r and the outer radius of the droplet, respectively. It is important to mention that the interface of a sessile

droplet was experimentally found and used as $h(r)$. Young's equation is a good approximation of the contact angle at the macro-scale;²³ however, it does not predict well experimental results in micro- and nano-scales. Thus, $h(r) = (0.00019^2 - r^2)^{1/2} - 0.00014$, which was

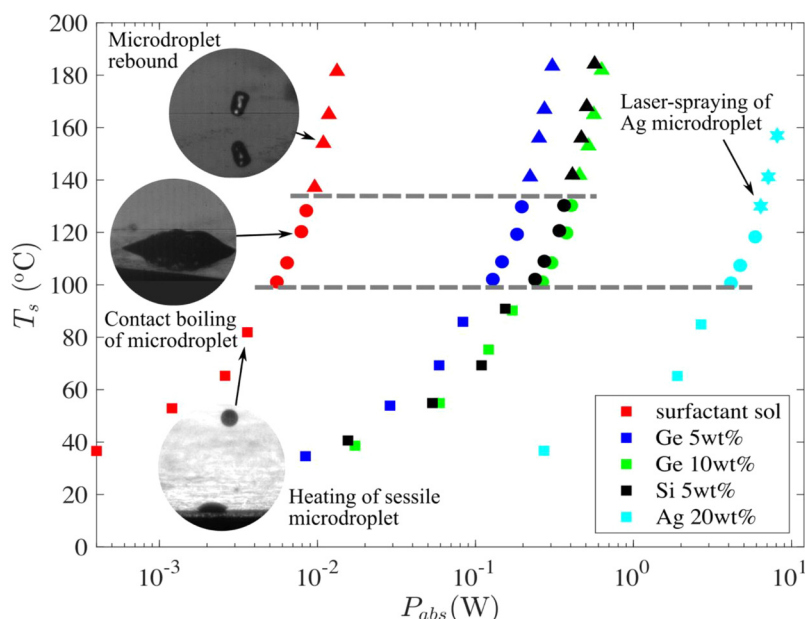


FIG. 4. Regime plot for laser-heated microdroplets carrying nanoparticles based on the impacting power absorbed by the microdroplets and the surface temperature of the substrate. Plot shows four different outcomes depending on the power absorbed by microdroplets and the surface temperature of a silicon substrate. Squares represent the cases where no boiling of droplet is observed, i.e., the heating of the sessile microdroplet regime; circles represent the cases where contact boiling is observed; and triangles where droplet rebound is observed due to film boiling. Finally, only for microdroplets of suspension Ag, 20 wt. %, a different regime was observed, i.e., the laser-spraying of the microdroplet.

found curve fitting the droplet interface as a spherical cap (supplementary material³⁴).

Results shown in Fig. 4 suggest that the transition to contact boiling regime occurs at $\sim 100^\circ\text{C}$. This occurs obviously because all the liquids tested were prepared by suspending nanoparticles in de-ionized (DI) water. At this temperature, the water starts to boil and the presence of nanoparticles promotes heterogeneous boiling. Heat is transferred by conduction from the solid substrate to the liquid microdroplet, while the entire droplet is additionally heated by the laser. The nanoparticles suspended in the liquid act as nuclei and vapor bubbles are generated at the nanoparticle surfaces. Moreover, the substrate temperature is increased as the laser power is increased, and this causes a more active heterogeneous nucleation that generates a pressure increase within the boiling droplet that finally produces bursting of vapor bubbles and ejection of liquid ligaments in the air. It must be noted that all microdroplets used have a concentration of the surfactant, and since the surface tension is lower to that of DI water alone, a lower heat flux is needed for the onset of nucleate boiling.²⁴

Contact boiling of the microdroplets of surfactant solution and semiconductor (Ge and Si) nanoparticles occur until certain surface temperature. After the surface temperature of the substrates exceeds a value of $\sim 138^\circ\text{C}$, the postcollision dynamics of the microdroplets is characterized for a restricted spreading of the liquid and a rapid recoil that does not allow the dissipation of its original kinetic energy. Subsequently, the microdroplet bounces back from the substrate. The bounced droplet recovers its spherical shape due to surface tension, reaches certain height until the kinetic and potential energies are balanced, and then falls down again onto the substrate.

This retraction and shape recovery of the microdroplet could be due partially to a decrease in the viscosity of the liquid at high

temperatures, which dampens the ability of the droplets to dissipate their kinetic energy, and the residual kinetic energy is stored in the droplet as potential energy. The upward bouncing of the droplets, on the other hand, may be due to localized rapid vaporization of the liquid at the point of contact between the droplet and the substrate, resulting in the Leidenfrost effect.^{19,20}

Film boiling happens after nucleate boiling and the minimum temperature for film boiling has a proportional dependence on the surface tension of the liquid.^{24,25} It should be noted that the contact boiling regime is produced by nucleate boiling of the water when the solid surfaces get hotter than the saturation temperature and that the Leidenfrost phenomenon is a special case of film boiling. The Leidenfrost temperature, which is the temperature at which the evaporation time of a drop reaches its maximum has been obtained experimentally by other researchers for different fluids and We numbers. Gottfried *et al.*⁵ found the Leidenfrost temperature to be $100\text{--}105^\circ\text{C}$ above the saturation temperature for carbon tetrachloride, ethanol, benzene, and n-octane impacting on a stainless steel plate. For water, he found that the exact value of the Leidenfrost temperature appears to depend upon the surface and the method of depositing the droplet and varied from 150 to 210°C above saturation and that it was independent of droplet size over the range studied. However, from the results obtained in this study, it can be seen that the onset of the droplet rebound regime (Fig. 4) is $\sim 138^\circ\text{C}$. If this phenomenon is caused by the Leidenfrost effect, it is happening at a much lower temperature than those reported in Ref. 5 and lower compared to temperatures reported by others. For instance, Tran *et al.*¹¹ reported transition between contact boiling and film boiling at $\sim 450^\circ\text{C}$ for $We = 32$ and $\sim 250^\circ\text{C}$ for $We = 2$. Henry²⁵ reported an approximated Leidenfrost temperature of 250°C for water on a hot copper surface. This discrepancy between these results may be due to the

fact that all drops in these studies have been produced by the action of gravity drawing liquid from a capillary tube (drop diameter ~ 2 mm); thus, the We number of drops is large compared to the We number used in this study, i.e., $We \sim 0.4$ since the diameter of droplets produced by the electrospray is $\sim 80 \mu\text{m}$. Furthermore, the Leidenfrost temperature has been shown to increase with the We number,^{26,27} which indicates that a lower surface temperature is necessary to keep the droplet impact at a low We number in film boiling. Therefore, the Leidenfrost effect may be producing droplet rebound at these lower surface temperatures.

Besides the heat transferred to the droplet by conduction through the vapor film on the lower part of the droplet, the laser Bessel beam irradiates the droplet on its upper part. Microdroplets have been shown to act as superlenses^{3,28,29} that can focus and enhance the intensity of an incident laser. Figure 2(b) contains an inset showing the intensity enhancement below a microdroplet of the surfactant solution. Therefore, the highest temperature within the droplet is located at the lowest part that promotes thermocapillary convection within the droplet to produce heating of the liquid that is not directly heated by the laser^{3,30} and a higher evaporation rate at the lower part of the droplet that accelerates the creation of a vapor layer beneath the droplet.

The characteristic vapor layer in the Leidenfrost phenomenon insulates the droplet from the hot solid surface; thus, the droplet does not experience nucleate boiling and bounces back because the vapor overpressure beneath the bottom surface overcomes the droplet's dynamic pressure, which has a direct relationship to its impacting We number^{31–33}. This vapor layer acts as a thin pressurized cushion within a small liquid-substrate gap that restricts the outflow of the vapor that is generated at the lower part of the droplet's outer surface. Finally, this overpressure propels the droplet upward away from the laser-focal spot. This phenomenon is detrimental if the objective is to deposit nanoparticles on the substrate since this inhibits the evaporation of the continuous liquid and subsequent sintering of nanoparticles on the substrate. Thus, the ability of delineating the transition between contact boiling and droplet rebound is fundamental for deposition and laser sintering of the nanoparticle (supplementary material³⁴).

Microdroplets of a 20 wt. % concentration Ag in DI water experienced a different phenomenon that is named in this study as the laser-spraying regime. Higher rates of heat transfer from the laser when these droplets are still in the air and on its way toward the substrate cause the disruption of the liquid outer surface. This disruption sometimes can even be explosive and disintegrates the original droplet, and subsequently, tinier liquid ligaments are ejected in the form of a narrow spray. In this regime, the original microdroplets do not reach the substrate to interact directly with the heated substrate; therefore, the surface temperature, T_s , has no effect on the dynamics of this phenomenon. Instead, the power absorbed by the microdroplet plays a major role since the radiation of energy causes vaporization of the liquid signaling a vapor pressure increase in the interior of the droplet.

When the physical properties of the precursor liquids are compared (Table I), it can be noted that the Ag, 20 wt. %, suspension varies significantly with the rest of the suspension in terms of reflectance and absorption coefficient at a wavelength 1064 nm. The reflectance and absorption coefficients are 6% and 100 cm^{-1} ,

respectively. Such a low reflectance indicates that only a small fraction of the incident laser energy is reflected and most of the energy is propagated within the droplet. Additionally, the absorption coefficient can be interpreted as the reciprocal of the penetration depth, which can be estimated to be $100 \mu\text{m}$. This value of penetration depth is in the same order of the average diameter of the droplets ($\sim 80 \mu\text{m}$), indicating that much of the laser energy is absorbed by the droplet and only a small amount of energy will heat up the substrate. In this regime, a spraying-like deposition of nanoparticles is achievable, which is convenient for flexible materials with a low melting temperature.

CONCLUSIONS

In this study, the thermal response of Bessel beam-heated microdroplets that carry semiconductor and metallic nanoparticles was investigated. Four different outcomes were identified in a phase diagram, showing the regimes: heating of the sessile droplet, contact boiling of the microdroplet, microdroplet rebound, and laser-spraying of the microdroplet. The transition between the first regime and the contact boiling (nucleate boiling phenomenon) is found to be at a surface temperature of $\sim 100^\circ\text{C}$. The transition between contact boiling and droplet rebound is found to be at $\sim 138^\circ\text{C}$. Microdroplets of 20 wt. % concentration of Ag in DI water experienced a different phenomenon, i.e., the laser-spraying regime. These transitions blemish the dependence of the Leidenfrost temperature on the solid surface for liquids with low reflectance and high absorption coefficient. Finally, the laser-microdroplet interactions influence the quality of nanoparticle deposition on a substrate.

ACKNOWLEDGMENTS

This work was supported by the National Science Foundation (NSF), CMMI, and MME (No. 1563448). The authors express special thanks to the UCF undergraduate students, Abhishek Sastri, and Marcos Barros for their assistance processing high-speed photographs.

REFERENCES

- 1 J. Thomas, P. Gangopadhyay, E. Araci, R. A. Norwood, and N. Peyghambarian, "Nanoimprinting by melt processing: An easy technique to fabricate versatile nanostructures," *Adv. Mater.* **23**, 4782–4787 (2011).
- 2 G. Niu and X. Chen, "When radionuclides meet nanoparticles," *Nat. Nanotechnol.* **13**, 359–360 (2018).
- 3 E. Castillo-Orozco, R. Kumar, and A. Kar, "Laser-induced subwavelength structures by microdroplet superlens," *Opt. Express* **27**, 8130–8142 (2019).
- 4 W. Chaze, O. Caballina, G. Castanet, J.-F. Pierson, F. Lemoine, and D. Maillat, "Heat flux reconstruction by inversion of experimental infrared temperature measurements—application to the impact of a droplet in the film boiling regime," *Int. J. Heat Mass Transfer* **128**, 469–478 (2019).
- 5 B. S. Gottfried, C. J. Lee, and K. J. Bell, "The Leidenfrost phenomenon: Film boiling of liquid droplets on a flat plate," *Int. J. Heat Mass Transfer* **9**, 1167–1188 (1966).
- 6 S. Chandra and C. T. Avedisian, "On the collision of a droplet with a solid surface," *Proc. R. Soc. London A* **432**, 13–41 (1991).
- 7 T. C. de Goede, K. G. de Bruin, N. Shahidzadeh, and D. Bonn, "Predicting the maximum spreading of a liquid drop impacting on a solid surface: Effect of surface tension and entrapped air layer," *Phys. Rev. Fluids* **4**, 053602 (2019).

- ⁸T. Mao, D. C. S. Kuhn, and H. Tran, "Spread and rebound of liquid droplets upon impact on flat surfaces," *AIChE J.* **43**, 2169–2179 (1997).
- ⁹A. Karl and A. Frohn, "Experimental investigation of interaction processes between droplets and hot walls," *Phys. Fluids* **12**, 785–796 (2000).
- ¹⁰H. Fujimoto, O. Yosuke, O. Tomohiro, and T. Hirohiko, "Hydrodynamics and boiling phenomena of water droplets impinging on hot solid," *Int. J. Multiphase Flow* **36**, 620–642 (2010).
- ¹¹T. Tran, H. J. J. Staat, A. Prosperetti, C. Sun, and D. Lohse, "Drop impact on superheated surfaces," *Phys. Rev. Lett.* **108**, 036101 (2012).
- ¹²J. D. Bernardin, C. J. Stebbins, and I. Mudawar, "Mapping of impact and heat transfer regimes of water drops impinging on polished surface," *Int. J. Heat Mass Transfer* **40**, 247–267 (1997).
- ¹³H. Chaves, A. M. Kubitzek, and F. Obermeier, "Dynamic processes occurring during the spreading of thin liquid films produced by drop impact on hot walls," *Int. J. Multiphase Flow* **20**, 470–476 (1999).
- ¹⁴N. Z. Mehdizadeh and S. Chandra, "Boiling during high-velocity impact of water droplets on a hot stainless steel surface," *Proc. R. Soc. London A* **462**, 3115–3131 (2006).
- ¹⁵E. Castillo-Orozco, R. Kumar, and A. Kar, "Laser electrospray printing of nanoparticles on flexible and rigid substrates," *J. Laser Appl.* **31**, 022015 (2019).
- ¹⁶W. Feng, Y. C. Wan, X. Shan, and H. Zheng, "Patterning of aluminium metalized pet film using high repetition rate fiber laser," *J. Laser Appl.* **31**, 022208 (2019).
- ¹⁷E. Castillo-Orozco, A. Kar, and R. Kumar, "Electrospray mode transition of microdroplets with semiconductor nanoparticle suspension," *Sci. Rep.* **7**, 5144 (2017).
- ¹⁸E. Castillo-Orozco, A. Kar, and R. Kumar, "Non-dimensional groups for electrospray modes of highly conductive and viscous nanoparticle suspensions," *Sci. Rep.* **10**, 4405 (2020).
- ¹⁹J. C. Burton, A. L. Sharpe, R. C. A. van der Veen, A. Franco, and S. R. Nagel, "Geometry of the vapor layer under a Leidenfrost drop," *Phys. Rev. Lett.* **109**, 074301 (2012).
- ²⁰F. Celestini, T. Frisch, and Y. Pomeau, "Take off of small leidenfrost droplets," *Phys. Rev. Lett.* **109**, 034501 (2012).
- ²¹D. McGloin and K. Dholakia, "Bessel beams: Diffraction in a new light," *Contemp. Phys.* **46**, 15–28 (2005).
- ²²M. A. Porras, C. Ruiz-Jiménez, and J. C. Losada, "Underlying conservation and stability laws in nonlinear propagation of axicon-generated Bessel beams," *Phys. Rev. A* **92**, 063826 (2015).
- ²³W. J. Jasper and N. Anand, "A generalized variational approach for predicting contact angles of sessile nano-droplets on both flat and curved surfaces," *J. Mol. Liq.* **281**, 196–203 (2019).
- ²⁴P. J. Berenson, "Film-boiling heat transfer from a horizontal surface," *J. Heat Transfer* **83**, 351–356 (1961).
- ²⁵R. E. Henry, "A correlation for the minimum film boiling temperature," *Chem. Eng. Prog. Symp. Ser.* **70**, 81–90 (1974).
- ²⁶S. Yao and K. Cai, "The dynamics and Leidenfrost temperature of drops impacting on a hot surface at small angles," *Exp. Therm. Fluid Sci.* **1**, 363 (1988).
- ²⁷J. Bernardin and I. Mudawar, "A Leidenfrost point model for impinging droplets and sprays," *J. Heat Transfer* **126**, 272 (2004).
- ²⁸V. N. Smolyaninova, I. I. Smolyaninov, A. V. Kildishev, and V. M. Shalaev, "Maxwell fish-eye and eaton lenses emulated by microdroplets," *Opt. Lett.* **35**, 3396–3398 (2010).
- ²⁹M. Duocastella, C. Florian, P. Serra, and A. Diaspro, "Sub-wavelength laser nanopatterning using droplet lenses," *Sci. Rep.* **5**, 16199 (2015).
- ³⁰D. Tam, V. von Arnim, G. H. McKinley, and A. E. Hosoi, "Marangoni convection in droplets on superhydrophobic surface," *J. Fluid Mech.* **642**, 101–123 (2009).
- ³¹G.-J. Michon, C. Josserand, and T. Séon, "Jet dynamics post drop impact on a deep pool," *Phys. Rev. Fluids* **2**, 023601 (2017).
- ³²A. Saha, Y. Wei, X. Tang, and C. Law, "Kinematics of vortex ring generated by a drop upon impacting a liquid pool," *J. Fluid Mech.* **875**, 842–853 (2019).
- ³³Y. Shen, S. Liu, C. Zhu, J. Tao, Z. Chen, H. Tao, L. Pan, G. Wang, and T. Wang, "Bouncing dynamics of impact droplets on the convex superhydrophobic surfaces," *Appl. Phys. Lett.* **110**, 221601 (2017).
- ³⁴See the supplementary material at <https://dx.doi.org/10.2351/7.0000332> with the Matlab script to compute the power absorbed by a microdroplet and for videos showing the dynamics of the Bessel beam-heated microdroplets.

Meet the Authors

Eduardo Castillo-Orozco is an Assistant Professor in Mechanical Engineering at Escuela Superior Politécnica del Litoral (ESPOL). His research interests are in the areas of Electrospray Nanoparticle Deposition, Droplet Impact, and Laser Additive Manufacturing.

Ranganathan Kumar leads the Two-Phase Flow and Microfluidic Laboratory at the University of Central Florida. His research interests are in the areas of Multiphase flow and heat transfer, Droplet atomization and vaporization, Microfluidics and nanofluids, Laser-based measurements, and CFD. He is a Fellow of ASME. In 2011, he received the prestigious Pegasus Professor award at the UCF.

Aravinda Kar is a Professor of Optics in CREOL, The College of Optics and Photonics. His research interests are Laser Advanced Manufacturing and Materials Processing. He is a Fellow of the Laser Institute of America and a Fellow of the National Academy of Inventors. He has co-authored a book entitled *Theory and Application of Laser Chemical Vapor Deposition*.